Deblending using robust inversion of Stolt-based Radon operators

Amr Ibrahim and Daniel Trad

ABSTRACT

In this report, we compare the denoising and inversion-based methods for deblending using Stolt-based Radon operators. These operators are used to construct a robust inversion problem with a sparsity constraint. Sparsity promoting transforms, such as Radon transform, can focus seismic data and produce a sparse model which can be used to separate signals, remove noise, or interpolate missing traces. For this reason, Radon transforms are a suitable tool for deblending. We can incorporate Radon transform into the deblending problem in two ways, either using denoising-based or an inversion-based approach. The denoising-based method treats blending interferences as random noise by sorting the data into new gathers, such as common receiver gathers. In these gathers, blending interferences exhibit random structures due to the randomization of the source firing times. On the other hand, the inversion-based method treats blending interferences as a signal, and the transformation can model this signal in the Radon domain by incorporating the blending operator to formulate an inversion problem. We compare both methods using sparse inversion in the hyperbolic Radon domain. Synthetic and field data examples show that the inversion-based approach can produce more accurate separation and better convergence. However, the inversion-based method increases the computational cost of deblending.

INTRODUCTION

Blended seismic acquisition is becoming a more appropriate technique to increase seismic illumination of the subsurface without increasing survey cost (Berkhout et al., 2008). Moreover, blended acquisition can reduce the need for interpolating seismic sources. However, unlike interpolation, increasing the total number of sources in the survey by employing blended acquisition introduce new information about the subsurface. Consequently, seismic images that use a denser source sampling should be more reliable than images estimated using interpolated sources. Furthermore, blended acquisition can introduce an added degree of freedom in survey design. For example, survey operators can vary the speed of seismic streamer boats or vibroseis vehicles without endangering the overall source density (Berkhout et al., 2008). Additionally, blended sources can reduce the cost and non-repeatability issues of time-lapse (4D seismic) survey (Ayeni et al., 2009; Krupovnickas et al., 2012; Wason et al., 2014). Time-lapse surveys repeat the 3D seismic acquisition of hydrocarbon reservoirs to monitor changes in the rock properties during production (Lumley, 2001). However, imaging artifacts due to non-repeatable seismic acquisition conditions can obscure the changes due to subsurface rock properties. Therefore, increasing the source sampling density by using blended acquisition can reduce these non-repeatability effects (Ayeni et al., 2009).

Separating blended sources is not a new topic for either impulsive seismic sources or marine seismic acquisition. However, early research was concerned with avoiding or removing these undesired sources. These sources were usually attributed to other seismic surveys shooting in nearby areas and commonly known as crew noise or cross talk. Lynn et al. (1987) presented an extensive study of seismic crew noise by analyzing datasets from the Gulf of Mexico and the North Sea. They concluded that these interferences could be treated as incoherent noise as long as the interfering seismic sources are not shooting in a synchronized fashion. In this case, the interfering signals appear as incoherent noise in common mid-point (CMP) gather. Therefore, conventional denoising algorithms can remove these asynchronous interferences by processing the data along different gathers such as common receiver gathers (CRG), common offset gathers (COG), or common mid-point gather (CMP).

We can group the deblending methods in literature into three main categories. The first category uses a conventional seismic processing sequence for blended data without separation. These passive deblending methods utilize the power of stacking in the traditional processing sequence to suppress source interferences. Standard stacking and migration algorithms could attenuate the incoherent source interferences enough to produce acceptable subsurface images. However, Stefani et al. (2007) and Spitz et al. (2008) noted that conventional processing and migration algorithms could be insufficient for some complicated datasets. Moreover, interferences can impact the accuracy of many pre-imaging steps, such as surface-related multiple eliminations (SRME). Additionally, Dragoset et al. (2009) and Abma et al. (2010) suggested that conventional processing cannot achieve the quality required for amplitude-dependent analysis such as AVO, time-lapse seismic, and fracture analysis.

The second category of deblending methods, treat interferences as noise, and use a denoising algorithm to remove them. For example, Moore et al. (2008) suggested using Radon transforms as a stacking tool to attenuate source interferences in common receiver gathers. Akerberg et al. (2008) also suggested that Radon transform combined with a sparse inversion scheme to enhance the source separation quality. Spitz et al. (2008) suggested using a prediction error filter (PEF) based subtraction to attenuate source interferences. Kim et al. (2009) suggested modeling the coherent interferences and adaptively subtracting them to preserve weak signals. Huo et al. (2009) suggested using a multi-dimensional vector-median filter to suppress the interferences robustly. Maraschini et al. (2012) used an iterative method based on rank reduction filtering to remove source interferences. Trad et al. (2012) suggested using the apex shifted Radon transform as a geometrical filter for sources in common shot gathers. Ibrahim and Sacchi (2014c); Ibrahim (2015) suggested using the apex shifted Radon transform within a robust denoising algorithm to remove source interferences and preserve weak signals in common receiver gathers. Sacchi (2014) redesigned a sparse Radon deblending that moves source interferences from the misfit term to the regularization term to avoid attenuating weak signals. This formulation improves the recovery of weak by excluding the fitting outliers caused by the source interferences from the misfit term. Ibrahim and Sacchi (2014b,a, 2015) suggested using migration/demigration operators (Trad, 2003) to speed up source separation using robust Radon transform.

The third category of deblending methods, treat interference as a signal, and cast the deblending problem as an inversion problem. In Berkhout (2008) blended sources framework, the firing times are contained in a blending operator. This operator is used to formulate an inversion problem for deblending. Similar to many inversion problems in geophysics, the deblending problem is ill-posed. Therefore, the inversion cost function should include a constraint to achieve a unique and stable solution. One of the most common and efficient constraints used in seismic data processing is the sparse inversion constraint. The sparsity constraint implies that the seismic data have a sparse (focused) representation in the chosen transform domain. In other words, the coherent seismic signals are stacked to significant amplitude coefficients, while the incoherent signals (noise) stack to near-zero coefficients in the transform domain. Therefore, in the inversion-based deblended methods rather than inverting directly for the deblended data, one can invert for the coefficients of the deblended data in the sparse transform domain. If we choose a suitable transform, we can estimate the deblended data from the sparse inverted model.

The choice of a suitable transform can be critical to the success of deblending algorithms that use sparsity constraints. Moore (2010) noted this connection between the efficiency of the sparsity-based source separation and the simplicity of subsurface geology. For example, a simple subsurface model results in seismic data that can transform into a sparse model. Therefore, including the sparsity constraint with a suitable sparsity promoting transform increases the quality of source separation. Mahdad et al. (2011) developed an iterative inversion algorithm that uses a coherency constraint in the Fourier domain to separate seismic sources. Van Borselen et al. (2012) developed an inversion-based deblending method that uses the constraint that nearby sources produce similar records. Wason et al. (2011) combined the inversion-based source separation problem with the compressive sensing problem to increase the survey efficiency. In this approach, the source separation and data interpolation problems are solved simultaneously. Wason et al. (2011) used the curvelet transform domain to impose the sparsity constraint on the inversion problem. Kontakis and Verschuur (2015) suggested combining coherency-based separation and sparse inversion-based source separation in the focal transform domain to improve the separation quality and reduce the dependency on model sparsity. Similarly, Cheng and Sacchi (2015) used rank reduction to solve for source separation and interpolation simultaneously.

THEORY

Radon transforms

Many applications use Radon transforms such as medical imaging, remote sensing and seismic data processing. In seismic data processing, Radon transform have been used for interpolation (Sacchi and Ulrych, 1995a; Trad et al., 2002; Ibrahim et al., 2018), multiple separation, denoising and microseismic signal detection (Sabbione et al., 2013). To derive the general formulation for Radon operators, let us assume that $d(t,x)$ denote the two dimensional seismic data and $m(\tau,\xi)$ denote the Radon model (Sacchi and Ulrych, 1995b). We first define the forward Radon operator, $\mathscr{L}$, and its adjoint operator $\mathscr{L}^\dagger$ as follow

$$d(t,x) = \mathscr{L}\; m(\tau,\xi) = \int_{-\infty}^{\infty} m(\tau = \phi\,(t,x,\xi),\xi)\; d\xi, \tag{1}$$

$$\widetilde{m}(\tau,\xi) = \mathscr{L}^\dagger\; d(t,x) = \int_{-\infty}^{\infty} d(t = \widetilde{\phi}\,(\tau,x,\xi),x)\; dx, \tag{2}$$

where $\widetilde{m}(\tau, \xi)$ is the Radon model estimated by the adjoint operator. The parameter ξ is the Radon parameter (or parameters) that define the Radon operator integration path by the function $\phi(\tau, x, \xi)$. Radon transform operators are adaptable, and they can use many different geometrical curves as their integration path. These different geometrical curves result in varieties of Radon transforms, which we can use in different data domains. When we process seismic data in common receiver gathers (CRG), seismic reflection travel times appear as apex shifted hyperbolas. Therefore, the apex shifted Radon transform (ASHRT) is the most suitable transform to focus CRG into a sparse Radon model. The following formulas describe the forward and adjoint ASHRT operators,

$$\phi(\tau, x, \xi) = \sqrt{t^2 - \frac{(x - x_0)^2}{v^2}} \tag{3}$$

$$\widetilde{\phi}(\tau, x, \xi) = \sqrt{\tau^2 + \frac{(x - x_0)^2}{v^2}}. \tag{4}$$

where the Radon parameters ξ are velocity v and apex location x_0. However, computing ASHRT operators in the time domain can be computationally prohibitive. Therefore, Trad (2003) suggested using Stolt migration operators in the $\omega - k$ domain to compute the ASHRT transform more efficiently. Also, Ibrahim and Sacchi (2015) used the Stolt-based Radon transform for denoising-based deblending.

Stolt-based Radon transform

The Stolt migration method is considered to be the fastest migration algorithm. This operator performs seismic migration by mapping data in the $\omega - k$ domain to vertical wavenumber k_z for a constant subsurface velocity. Despite not being widely used anymore in seismic imaging due to its constant velocity limitation, the low computational cost of the Stolt operator made it a useful tool in other fields such as medical imaging and synthetic aperture radar imaging. Using the exploding reflector principle (Claerbout, 1985) and a constant velocity assumption, the Stolt operator, can be used to estimate the subsurface model from zero-offset data. This estimated model $\widetilde{m}(\tau, v, x)$ is related to the data recorded at the surface $d(t, x)$ by the following relationship (Yilmaz, 2001)

$$\widetilde{m}(\tau, v, x) = \int\int d(\omega, k_x)\ \exp[-ik_x x - i\omega_\tau(v)\tau]\, d\omega\, dk_x, \tag{5}$$

where x represents the horizontal axis and ω_τ is the Fourier dual of the apex time τ which is a function of the velocity through the modified dispersion relationship (Yilmaz, 2001)

$$\omega_\tau = \sqrt{\omega^2 - (vk_x)^2}. \tag{6}$$

Equation 5 can be rewritten by changing the integration variable from ω to ω_τ

$$\widetilde{m}(\tau, v, x) = \int\int C\ d(\omega = \sqrt{\omega_\tau^2 + (vk_x)^2}, k_x) \times \exp\left[-ik_x x - i\omega_\tau(v)\tau\right] d\omega_\tau\, dk_x, \tag{7}$$

where $C = \omega_\tau/\omega$ is a scaling factor resulting from the change of variables. Similarly, the forward Stolt modelling operator can be written as

$$d(t,x) = \int\int\int m(\omega_\tau = \sqrt{\omega^2 - (vk_x)^2}, v, k_x) \times \exp[ik_x x + i\omega t]\; d\omega\; dk_x\; dv. \quad (8)$$

The forward and adjoint transforms in equations (7) and (8) can be written in operator form as follows

$$\mathbf{L}^T = \mathbf{F}^{-1}_{\omega_\tau,k_x}\; \mathbf{M}^T_{\omega,v,k_x}\; \mathbf{F}_{t,x}\; \mathbf{S}^T, \quad (9)$$

$$\mathbf{L} = \mathbf{S}\; \mathbf{F}^{-1}_{\omega,k_x}\; \mathbf{M}_{\omega_\tau,v,k_x}\; \mathbf{F}_{\tau,x}, \quad (10)$$

where, $\mathbf{F}$ is the Fourier transform, $\mathbf{M}_{\omega_\tau,v,k_x}$ is the Stolt mapping operator and $\mathbf{S}$ is a summation operator and its adjoint is a spraying operator (Claerbout, 1985). Although we derive the Stolt operator with a constant velocity assumption, it can be used to construct an equivalent of the ASHRT model with multiple velocities. Since each image represents one plane inside the ASHRT cube at a constant velocity, then the ASHRT model is a collection of all these images. Therefore, the adjoint Stolt operator in equation 9 includes a spreading operator $\mathbf{S}^T$ that computes several images with different velocities from the same data while the forward Stolt operator in equation 10 uses a summation operator to model the data.

Robust inversion

We can assume that the common receiver gather is contaminated with noise (source interferences). Therefore, we pose the problem of estimating a noise free Radon model $\mathbf{m}$ of this gather as an inversion problem. To solve this problem, we minimize the residual between the observed data and the modelled data,

$$\mathbf{r} = \mathbf{d} - \mathbf{L}\,\mathbf{m}, \quad (11)$$

where $\mathbf{d}$ is the common receiver gather data contaminated with interferences, $\mathbf{L}$ is the Radon modelling operator and $\mathbf{m}$ is the estimated Radon model. This problem is an ill-posed inversion (Sacchi and Ulrych, 1995a). Therefore, a regularization term must be included in the inversion cost function to estimate a unique and stable model. Therefore, the Radon transform inversion problem can be formulated by minimizing the following general cost function

$$\begin{aligned} J =& \|\mathbf{r}\|_p^p + \mu\|\mathbf{m}\|_q^q \\ =& \|\mathbf{d} - \mathbf{L}\,\mathbf{m}\|_p^p + \mu\|\mathbf{m}\|_q^q, \end{aligned} \quad (12)$$

where the first term on the right hand side is the misfit term and the second term is the regularization term. In both terms we assume that ℓ_p and ℓ_q norms are given by the general expressions $\ell_p = \sum_i |r_i|^p$ and $\ell_q = \sum_i |m_i|^q$. The parameters p and q represent the exponent of the p-norm of the misfit and the $q-$norm of the model regularization term, respectively. We conventionally use ℓ_2 norm ($p = 2$) for the misfit (least-squares inversion) with the implicit assumption that the fitting errors are small and follow a Gaussian probability distribution. However, if the data contain strong noise that does not follow a

Gaussian probability distribution, minimizing the ℓ_2 misfit should produce a biased model due to the strong fitting outliers (Ibrahim and Sacchi, 2014c; Ibrahim, 2015). Therefore, we should use a ℓ_1 norm ($p = 1$) misfit when there are strong fitting outliers such as source interferences in common receiver gathers. Using the ℓ_1 norm misfit is commonly known as robust inversion since it is more robust to fitting outliers than the conventional ℓ_2 norm misfit. Moreover, to fairly compare the denoising-based and inversion-based methods, we use robust inversion for both of them. The inversion cost function is minimized using Iteratively Reweighted Least Squares (IRLS) algorithm. For more details regarding IRLS, please refer to Daubechies et al. (2010); Trad et al. (2003); Ibrahim and Sacchi (2014c).

DEBLENDING METHODS

Denoising-based deblending

The denoising-based deblending employs the incoherency of source interferences due to the spatial source separation and the dithering (random delays) of firing times. Deblending assumes that blended source data can be modeled from its single-source components. For example, if we let $\mathbf{D}$ represents the data of all single sources in the time-space domain arranged into a data cube and $\mathbf{b}$ represents the two-dimensional blended sources data, then

$$\mathbf{b} = \mathbf{\Gamma}\,\mathbf{D}, \tag{13}$$

where $\mathbf{\Gamma}$ represents the blending operator that contains the source coding information (firing times and spatial locations) (Berkhout, 2008). Therefore, blended data $\mathbf{b}$ can be separated by compensating for the source firing delays and subdividing of the data into single-source segments. This operation is commonly known as pseudo-deblending. Pseudo-deblending is equivalent to applying the adjoint of the blending operator $\mathbf{\Gamma}^T$ to the blended data $\mathbf{b}$ such that

$$\widetilde{\mathbf{D}} = \mathbf{\Gamma}^T\mathbf{b}, \tag{14}$$

where $\widetilde{\mathbf{D}}$ represents the pseudo-deblended data cube. Pseudo-deblending does not remove source interferences. However, source interferences exhibit an incoherent structure in common receiver gathers due to the time dithering of source firing times. Therefore, a denoising algorithm can be used to attenuate source interferences and achieve deblending.

In the denoising-based deblending, we assume that the common receiver gather, which is equivalent to common shot gather due to reciprocity, is contaminated with blending noise (source interferences). Therefore, we can pose the deblending problem as the problem of estimating a noise-free Radon model $\mathbf{m}$ of the common receiver gather. We can cast Radon denoising as an inversion problem that minimizes the residual between the observed (noisy) CRG gather and the modeled (noise-free) CRG gather,

$$\mathbf{r} = \widetilde{\mathbf{D}} - \mathbf{L}\,\mathbf{m}, \tag{15}$$

where, $\widetilde{\mathbf{D}}$ is the pseudo deblended data cube similar to equation 14, $\mathbf{L}$ is the Radon modeling operator and $\mathbf{m}$ is the estimated Radon models for all common receiver gathers in the data. A regularization term must be added to the cost function in equation 15 to estimate a noise-free, unique, and stable model. Therefore, we reformulate the Radon denoising problem to a robust inversion problem with sparse regularization expressed by the following cost function

$$J = \|\widetilde{\mathbf{D}} - \mathbf{L}\,\mathbf{m}\|_1^1 + \mu\|\mathbf{m}\|_1^1, \tag{16}$$

Inversion-based deblending

In the framework proposed by Berkhout (2008), the blending operator contains the sources firing times and locations. This operator can be used to formulate an inversion problem for deblending such as

$$J = \|\mathbf{b} - \mathbf{\Gamma D}\|_1^1, \tag{17}$$

where again, $\mathbf{\Gamma}$ is the blending operator, and similar to the denoising-based deblending, $\mathbf{b}$ is the blended data, and $\mathbf{D}$ is the separate shots data cube. It is clear that this inversion problem is ill-posed, and minimizing the cost function do not produce the deblended shots. Therefore, we must include an inversion constraint. To utilize the power of Radon transform sparsity, we can rewrite the cost function as

$$J = \|\mathbf{b} - \mathbf{\Gamma L m}\|_1^1 + \mu\|\mathbf{m}\|_1^1, \tag{18}$$

where $\mathbf{L}$ and $\mathbf{m}$ are the Radon operator, and Radon model of all common receiver gathers similar to the denisoing based approach. The deblended shots should be estimated from the Radon model $\mathbf{m}$ by the forward modeling operator.

There are two main differences between the cost functions in equations 16 and 18. First, the inversion-based deblending cost function includes the blending the operator $\mathbf{\Gamma}$ into the inversion while the denoising-based does not use it. Second, the denoising-based deblending cost function 16 used the pseudo-deblended $\widetilde{\mathbf{D}}$ as the observed data while the inversion-based cost function uses the blended shots $\mathbf{b}$ as the observed data. These two differences lead to two significant conclusions. The first is that the blending operator in equation 18 would increase the computation cost since it needs all the blended shots as input. The second is that the misfit term in equation 18 represents the small fitting errors between the observed the modeled blended shot while the misfit term in equation 16 contains the source interferences which have large amplitudes and incoherent structure.

EXAMPLES

Synthetic Example

We test our deblending method using a numerically blended synthetic data set. The synthetic data were modeled using finite-difference modeling of the marmousi model using a Ricker wavelet of the central frequency of $15Hz$ as a source. The acquisition scenario represents two source boats firing near simultaneously. The source firing times are dithered using random time delays to make the source interferences appear incoherent, Figure 1 shows the sources firing times for both conventional and blended acquisitions. The results of the denoising-based and inversion-based deblending are shown in Figure 2 and 3, respectively. These figures show a clear advantage for the inversion-based deblending over the denoising-based method.

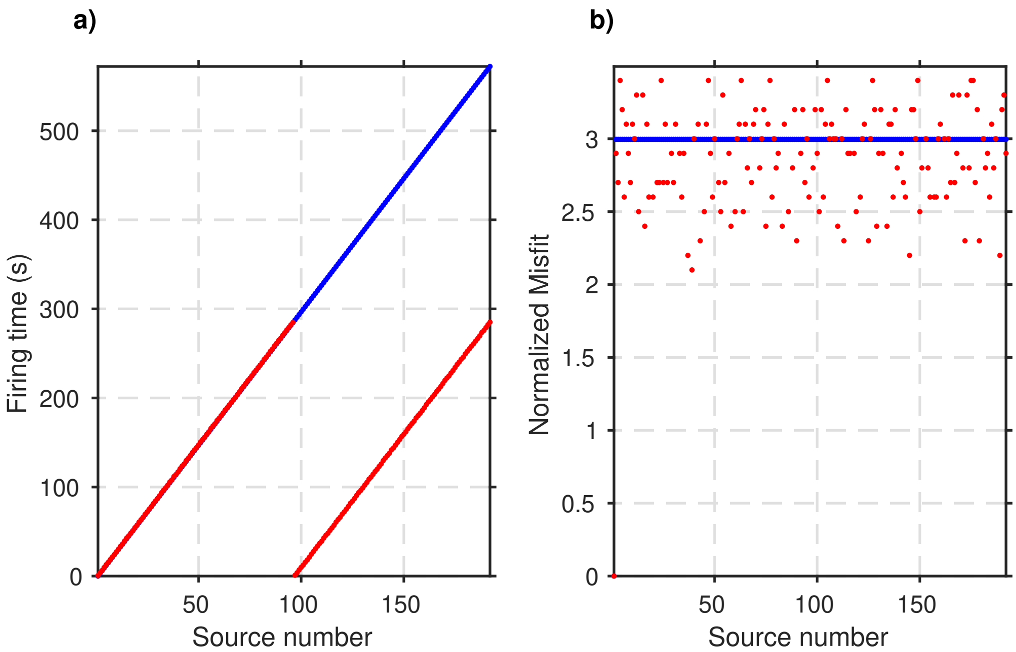

FIG. 1. Seismic sources firing times for Marmousi data example. (a) Firing times of conventional (blue) and simultaneous seismic sources (red). (b) Time delay between successive sources for conventional (blue) and simultaneous sources (red).

Field Data Example

We also tested the deblending methods using numerically blended marine data from the Mississippi Canyon area in the Gulf of Mexico. In this example, the acquisition simulates a single source boat traveling with a speed of about four times the normal speed. Therefore, four blended shots overlap in the time window of a conventional shot. Moreover, the dithering of the sources is limited to simulate the operational constraints in a marine acquisition. Figure 4 shows the firing times of the blended sources. This figure shows the limited randomization of the source firing times, which reduces the incoherency of the source interferences in common receiver gathers and makes the deblending more challenging. The results of the denoising-based and inversion-based deblending are shown in Figure 5 and 6, respectively. Again, these figures show a clear advantage for the inversion-based deblending over the denoising-based method.

CONCLUSIONS

We have implemented an inversion-based deblending method that uses robust inversion of Stolt-based Radon transform. We demonstrated that the inversion-based approach is better in deblending, especially in acquisition scenarios where operational constraints limit the dithering of the source firing times. However, the inversion-based deblending can require more computational resources, especially memory requirements, since it uses the blending operator in the inversion cost function. Therefore, computationally efficient transforms such as Stolt-based Radon transform can be beneficial in expanding the inversion-based deblending to 3D acquisition.

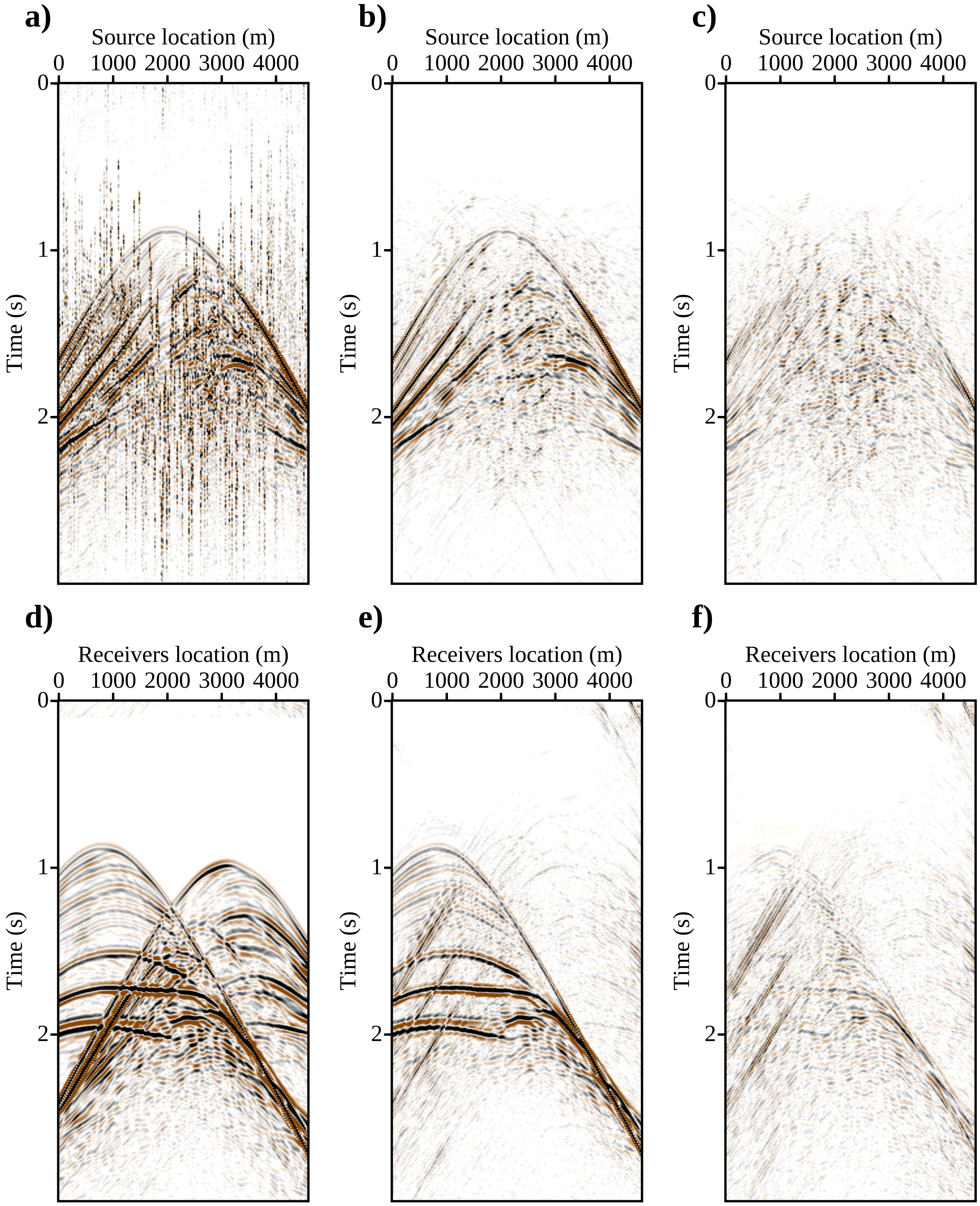

FIG. 2. Marmousi data example deblended using denoising approach. (a) Pseudo-deblended common receiver gather . (b) Noise-based deblended common receiver gather. (c) Deblending error of common receiver gather. (d) Pseudo-deblended common source gather. (e) Noise-based deblended common source gather. (f) Deblending error of common source gather.

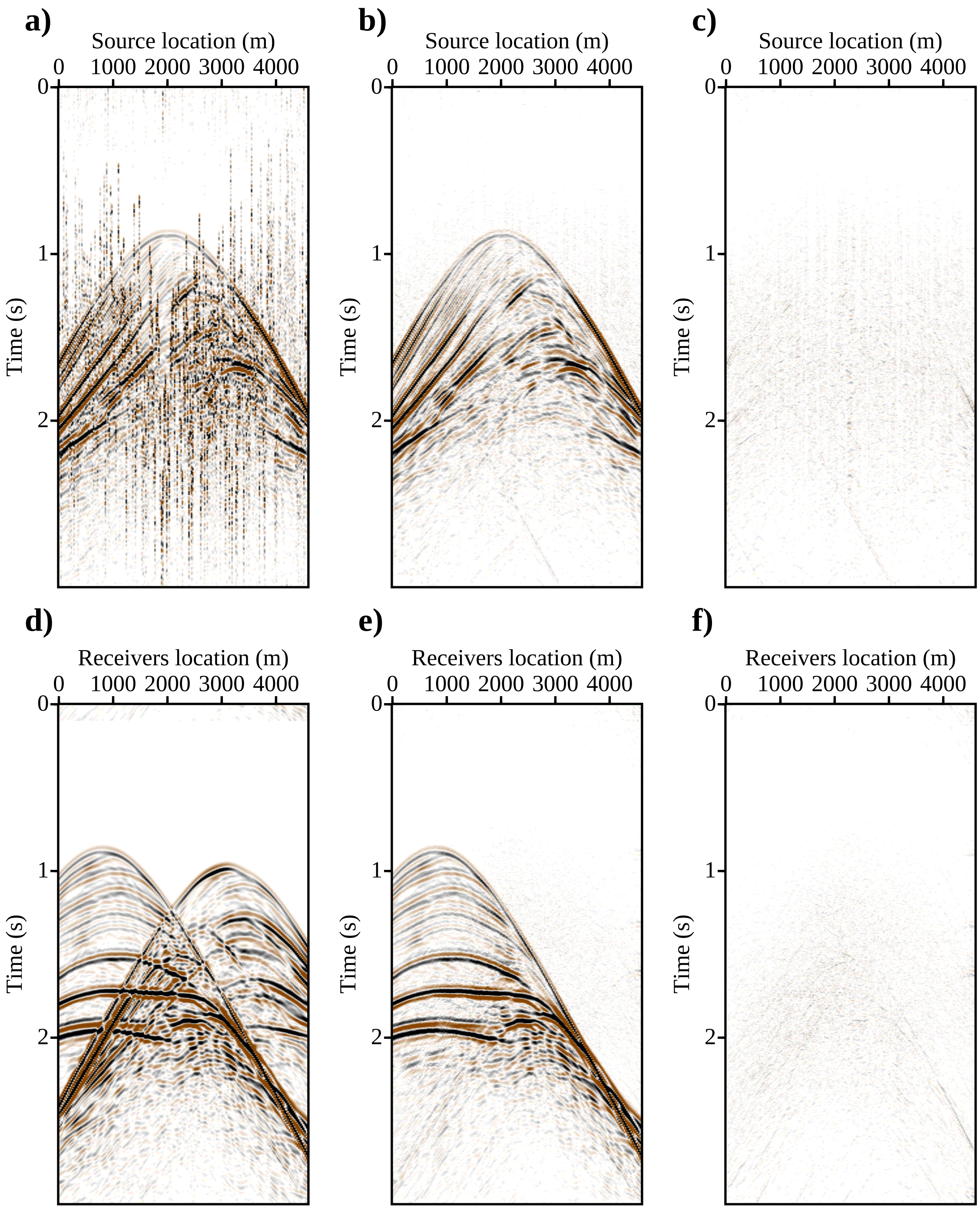

FIG. 3. Marmousi data example deblended using inversion approach. (a) Pseudo-deblended common receiver gather. (b) Inversion-based deblended common receiver gather. (c) Deblending error of common receiver gather. (d) Pseudo-deblended common source gather. (e) Inversion-based deblended common source gather. (f) Deblending error of common source gather.

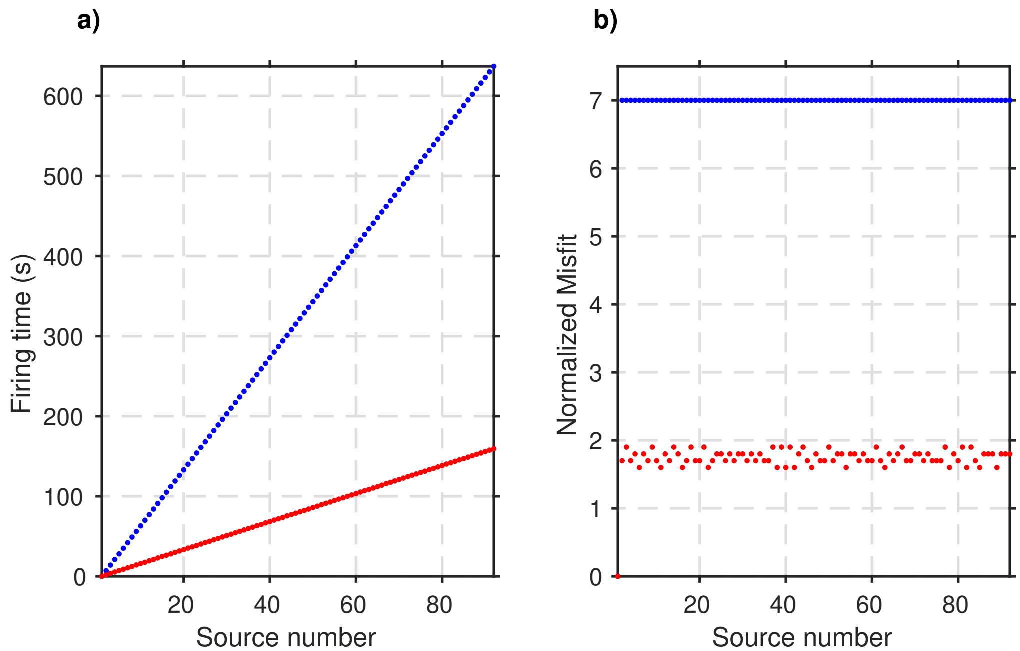

FIG. 4. Sources firing times for Gulf of Mexico data example. (a) Firing times of conventional (blue) and simultaneous seismic sources (red). (b) Time delay between successive sources for conventional (blue) and simultaneous sources (red).

ACKNOWLEDGMENTS

We thank the sponsors of CREWES for continued support. This work was funded by CREWES industrial sponsors and NSERC (Natural Science and Engineering Research Council of Canada) through the grant CRDPJ 461179-13.

REFERENCES

Abma, R., Manning, T., Tanis, M., Yu, J., and Foster, M., 2010, High quality separation of simultaneous sources by sparse inversion: 72nd Annual International Conference and Exhibition, EAGE, Expanded Abstracts, B003.

Akerberg, P., Hampson, G., Rickett, J., Martin, H., and Cole, J., 2008, Simultaneous source separation by sparse Radon transform: 78th Annual International Meeting, SEG, Expanded Abstracts, 2801–2805.

Ayeni, G., Tang, Y., and Biondi, B., 2009, Joint preconditioned least-squares inversion of simultaneous source time-lapse seismic data sets: 79th Annual International Meeting, SEG, Expanded Abstracts, 3914–3918.

Berkhout, A., 2008, Changing the mindset in seismic data acquisition: The Leading Edge, **27**, No. 7, 924–938.

Berkhout, A. J., Blacquière, G., and Verschuur, E., 2008, From simultaneous shooting to blended acquisition: 78th Annual International Meeting, SEG, Expanded Abstracts, 2831–2838.

Cheng, J., and Sacchi, M. D., 2015, Separation and reconstruction of simultaneous source data via iterative rank reduction: Geophysics, **80**, No. 4, V57–V66.

Claerbout, J., 1985, Imaging the Earth's Interior: Blackwell Scientific Publications Inc.

Daubechies, I., DeVore, R., Fornasier, M., and Güntürk, C. S., 2010, Iteratively reweighted least squares minimization for sparse recovery: Communications on Pure and Applied Mathematics, **63**, No. 1, 1–38.

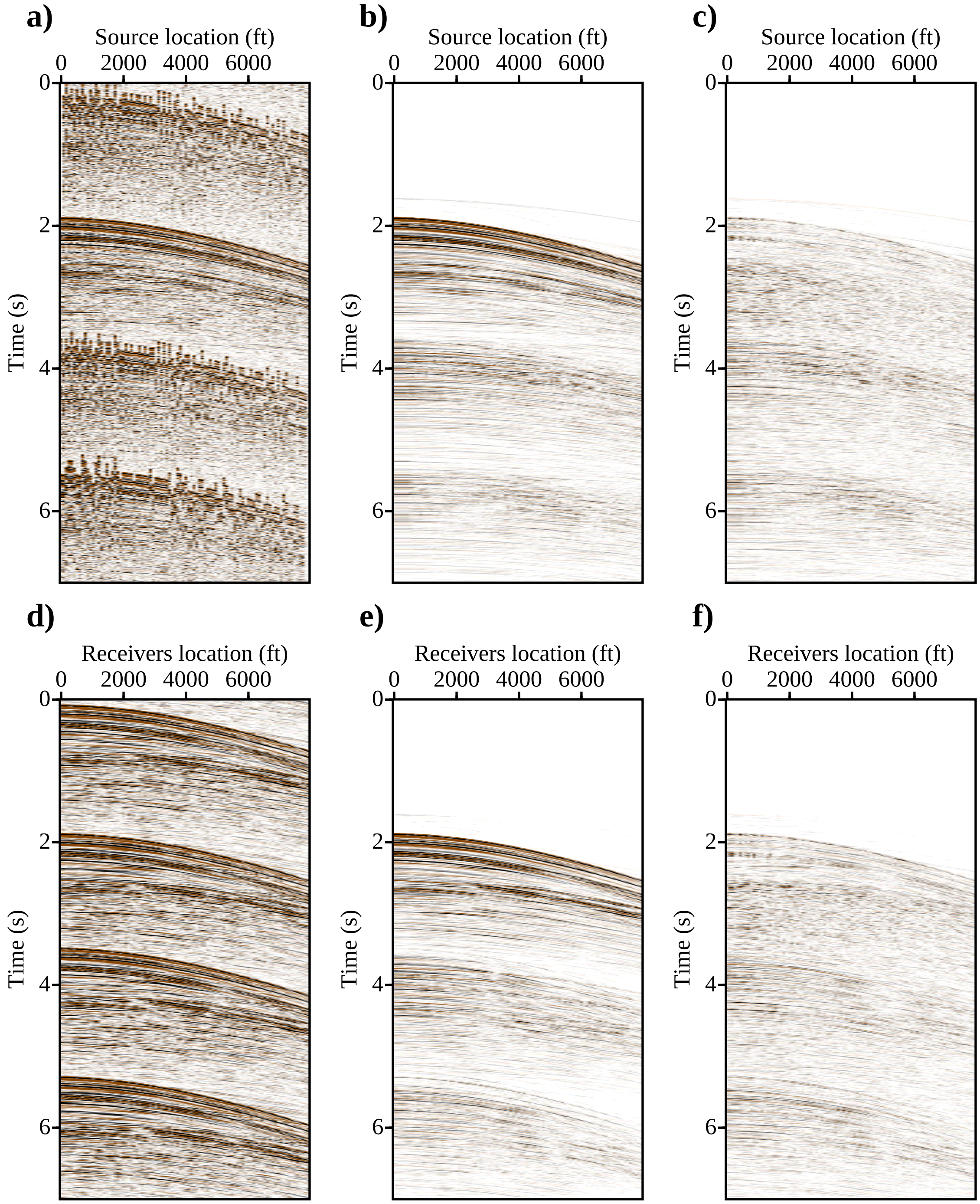

FIG. 5. Gulf of Mexico data example deblended using denoising approach. (a) Pseudo-deblended common receiver gather. (b) Noise-based deblended common receiver gather. (c) Deblending error of common receiver gather. (d) Pseudo-deblended common source gather. (e) Noise-based deblended common source gather. (f) Deblending error of common source gather.

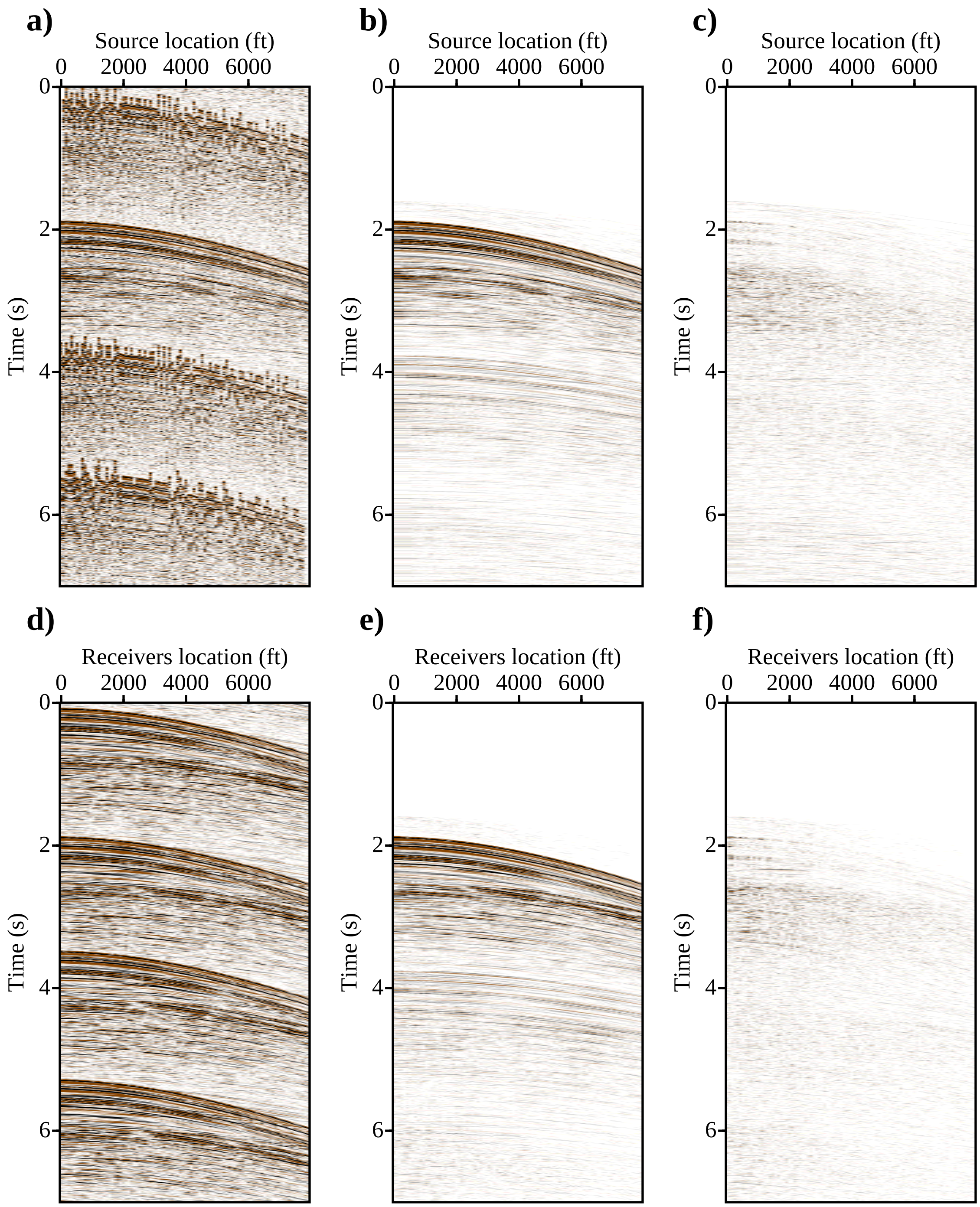

FIG. 6. Gulf of Mexico data example deblended using inversion approach. (a) Pseudo-deblended common receiver gather. (b) Inversion-based deblended common receiver gather. (c) Deblending error of common receiver gather. (d) Pseudo-deblended common source gather. (e) Inversion-based deblended common source gather. (f) Deblending error of common source gather.

Dragoset, W., Li, H., Cooper, L., Eke, D., Kapoor, J., Moore, I., and Beasley, C., 2009, A 3D wide-azimuth field test with simultaneous marine sources: 71st Annual International Conference & Exhibition, EAGE, Expanded Abstracts.

Huo, S., Luo, Y., and Kelamis, P., 2009, Simultaneous sources separation via multi-directional vector-median filter: International Annual Meeting, SEG, Expanded Abstracts, 31–35.

Ibrahim, A., 2015, Separating simultaneous seismic sources using robust inversion of Radon and migration operators: PhD Thesis, University of Alberta.

Ibrahim, A., and Sacchi, M. D., 2014a, Accelerating robust Radon transforms via the Stolt operator for simultaneous source separation: 84th Annual International Meeting, SEG, Expanded Abstracts, 202–207.

Ibrahim, A., and Sacchi, M. D., 2014b, Eliminating blending noise using fast apex shifted hyperbolic Radon transform: 76th Annual International Conference and Exhibition, EAGE, Expanded Abstracts, –.

Ibrahim, A., and Sacchi, M. D., 2014c, Simultaneous source separation using a robust Radon transform: Geophysics, **79**, No. 1, V1–V11, `http://library.seg.org/doi/pdf/10.1190/geo2013-0168.1`.

Ibrahim, A., and Sacchi, M. D., 2015, Fast simultaneous seismic source separation using Stolt migration and demigration operators: Geophysics, **80**, No. 6, WD27–WD36.

Ibrahim, A., Terenghi, P., and Sacchi, M. D., 2018, Simultaneous reconstruction of seismic reflections and diffractions using a global hyperbolic radon dictionary: Geophysics, **83**, No. 6, V315–V323.

Kim, Y., Gruzinov, I., Guo, M., and Sen, S., 2009, Source separation of simultaneous source OBC data: 79th Annual International Meeting, SEG, Expanded Abstracts, 51–55.

Kontakis, A., and Verschuur, D. J., 2015, Combined focal and coherency-based deblending strategy: 85th Annual International Meeting, SEG, Expanded Abstracts, 4667–4672.

Krupovnickas, T., Matson, K., Corcoran, C., and Pascual, R., 2012, Marine simultaneous source OBS survey suitability for 4D analysis: 82th Annual International Meeting, SEG, Expanded Abstracts, 1–5.

Lumley, D. E., 2001, Time-lapse seismic reservoir monitoring: Geophysics, **66**, No. 1, 50–53.

Lynn, W., Doyle, M., Larner, K., and Marschall, R., 1987, Experimental investigation of interference from other seismic crews: Geophysics, **52**, No. 11, 1501–1524.

Mahdad, A., Doulgeris, P., and Blacquiere, G., 2011, Separation of blended data by iterative estimation and subtraction of blending interference noise: Geophysics, **76**, No. 3, Q9–Q17.

Maraschini, M., Dyer, R., Stevens, K., and Bird, D., 2012, Source separation by iterative rank reduction-theory and applications: 74th Annual International Conference and Exhibition, EAGE, Expanded Abstracts.

Moore, I., 2010, Simultaneous sources–processing and applications: 72nd Annual International Conference & Exhibition, EAGE, Expanded Abstracts.

Moore, I., Dragoset, B., Ommundsen, T., Wilson, D., Ward, C., and Eke, D., 2008, Simultaneous source separation using dithered sources: 78th Annual International Meeting, SEG, Expanded Abstracts, 2806–2810.

Sabbione, J., Velis, D., and Sacchi, M. D., 2013, Microseismic data denoising via an apex-shifted hyperbolic Radon transform: 83th Annual International Meeting, SEG, Expanded Abstracts, 2155–2161.

Sacchi, M., and Ulrych, T., 1995a, High-resolution velocity gathers and offset space reconstruction: Geophysics, **60**, No. 4, 1169–1177.

Sacchi, M., and Ulrych, T., 1995b, Improving resolution of Radon operators using a model re-weighted least squares procedure: Journal of Seismic Exploration, **4**, 315–328.

Sacchi, M. D., 2014, Sparse inversion of the Radon coefficients in the presence of erratic noise with application to simultaneous seismic source processing, *in* 2014 IEEE International Conference on Acoustics, Speech, and Signal Processing (ICASSP), IEEE.

Spitz, S., Hampson, G., and Pica, A., 2008, Simultaneous source separation: A prediction-subtraction approach: 78th Annual International Meeting, SEG, Expanded Abstracts, 2811–2815.

Stefani, J., Hampson, G., and Herkenhoff, E., 2007, Acquisition using simultaneous sources: 69th Annual International Conference and Exhibition, EAGE, Expanded Abstracts.

Trad, D., 2003, Interpolation and multiple attenuation with migration operators: Geophysics, **68**, No. 6, 2043–2054.

Trad, D., Siliqi, R., Poole, G., and Boelle, J., 2012, Fast and robust deblending using apex shifted Radon transform: 82nd Annual International Meeting, SEG, Expanded Abstracts, **741**, 1–5.

Trad, D., Ulrych, T., and Sacchi, M., 2003, Latest views of the sparse Radon transform: Geophysics, **68**, No. 1, 386.

Trad, D. O., Ulrych, T. J., and Sacchi, M. D., 2002, Accurate interpolation with high-resolution time-variant Radon transforms: Geophysics, **67**, No. 2, 644–656.

Van Borselen, R., Baardman, R., Martin, T., Goswami, B., and Fromyr, E., 2012, An inversion approach to separating sources in marine simultaneous shooting acquisition – application to a gulf of mexico data set: Geophysical Prospecting, **60**, No. 4, 640–647.

Wason, H., Herrmann, F. J., and Lin, T. T. Y., 2011, Sparsity-promoting recovery from simultaneous data: A compressive sensing approach: 81st Annual International Meeting, SEG, Expanded Abstracts, 6–10.

Wason, H., Oghenekohwo, F., and Herrmann, F. J., 2014, Randomization and repeatability in time-lapse marine acquisition: 84th Annual International Meeting, SEG, Expanded Abstracts, 46–51.

Yilmaz, O. g., 2001, Seismic data analysis : processing, inversion, and interpretation of seismic data, Investigations in geophysics: Society of Exploration Geophysicists, Tulsa, OK, 2nd edn.